

Characterisation of poly(neutral red) modified carbon film electrodes; application as a redox mediator for biosensors

Rasa Pauliukaite · Mariana Emilia Ghica ·
Madalina Barsan · Christopher M. A. Brett

Received: 29 September 2006 / Revised: 15 December 2006 / Accepted: 23 January 2007 / Published online: 16 March 2007
© Springer-Verlag 2007

Abstract The polymer redox mediator, poly(neutral red) (PNR), has been synthesised and characterised electrochemically to investigate the best electropolymerisation and mediation conditions for application in enzyme biosensors and to clarify the mechanism of action. Neutral red was electropolymerised by potential cycling on carbon film electrode substrates by allowing the monomer to be oxidised during the full 20 cycles of polymerisation or reducing the positive limit of the potential window after the first 2 cycles to impede monomer oxidation with a view to obtaining longer polymer chains and a lesser degree of branching. Comparison was made with glassy carbon substrates. The PNR films on carbon film electrodes were characterised using cyclic voltammetry and electrochemical impedance spectroscopy, as well as in glucose biosensors prepared with PNR. Glucose oxidase enzyme was immobilised by encapsulation in silica sol-gel and compared with that obtained by cross-linking with glutaraldehyde. The biosensors were evaluated by chronoamperometry in 0.1 M phosphate buffer saline solution, pH 7.0, and showed evidence of electron transfer between the enzyme cofactor flavin adenine dinucleotide and PNR dissolved in the enzyme layer competing with PNR-mediated electrochemical degradation of H₂O₂ formed during the enzymatic process.

Keywords Poly(neutral red) · Electropolymerisation · Silica sol-gel · Enzyme immobilisation · Electrochemical impedance spectroscopy

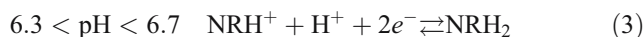
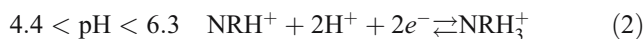
This paper is dedicated to Professor Dr. Algirdas Vaskelis on the occasion of his 70th birthday.

R. Pauliukaite · M. E. Ghica · M. Barsan · C. M. A. Brett (✉)
Departamento de Química, Universidade de Coimbra,
3004-535 Coimbra, Portugal
e-mail: brett@ci.uc.pt

Introduction

The phenazine dye, neutral red (NR; *N*⁸,*N*⁸,3-trimethylphenazine-2,8,-diamine), Fig. 1a, is used for a variety of purposes such as biological staining [1] for medical purposes to investigate viruses [2], as a pH indicator in biochemical systems [3], in the determination of DNA using optical and electrochemical methods [4], etc. Like other phenazine compounds, NR is electroactive and can be oxidised electrochemically. However, only a few reports have been published concerning electrochemical studies of NR [5, 6].

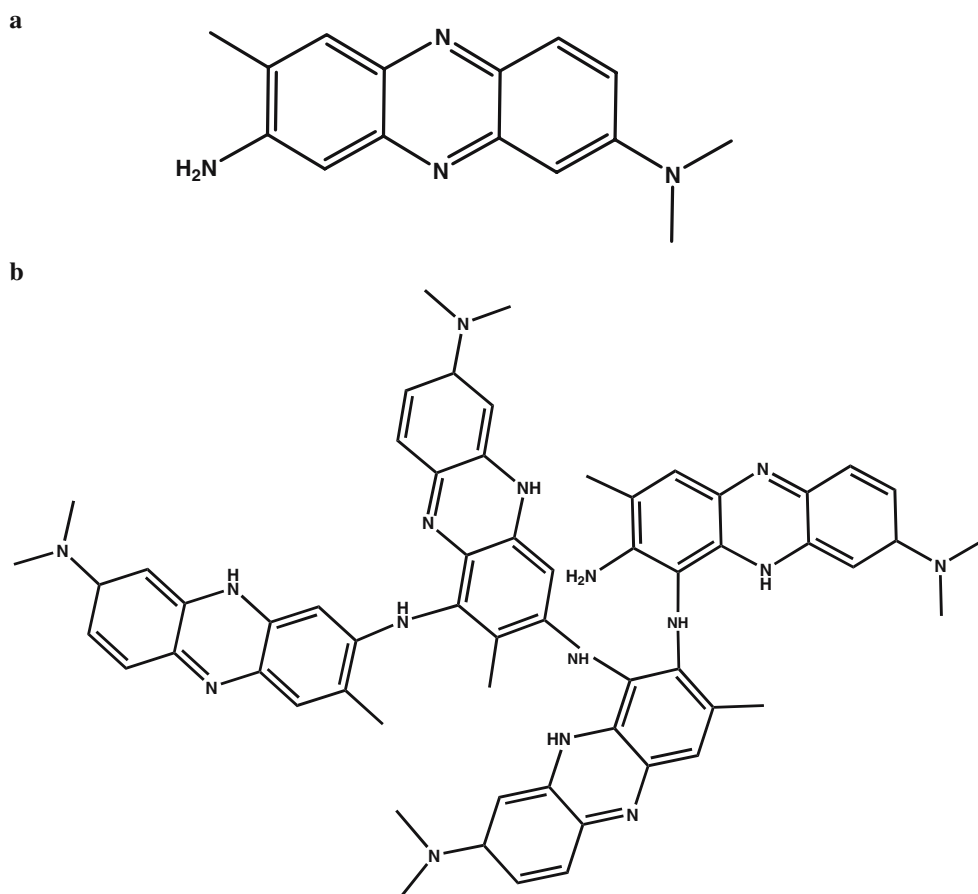
The electrochemistry of NR is strongly dependent on solution acidity. Protonation of NR and leuco-NR varies according to the pH [5]:



where NR is neutral red and NRH₂ represents leuco-NR.

Leuco-NR can be oxidised further and form radicals [6]. These radicals are unstable and easily react with each other leading to oligomers and polymers [7]—a possible structure of a tetramer is indicated in Fig. 1b. Electropolymerisation of NR and the electrochemical behaviour of poly(neutral red) (PNR) have been studied during the last decade [7–15], and PNR has been shown to have a rather similar behaviour to NR (Eqs. 1–4). It was also observed that PNR can interact with some biologically active compounds such as

Fig. 1 Structure of **a** neutral red ($N^8, N^8, 3$ -trimethylphenazine-2,8,-diamine) and **b** possible chemical structure of a tetramer



nicotinamide adenine dinucleotide (reduced form) [7, 9, 16], nitric oxide [17], dopamine, ascorbic acid [18], citrate [19], and heparin [20].

Recently, PNR has been used as a redox mediator in electrochemical biosensors [21–24]. In [21–23], carbon film electrodes prepared from electrical resistors [25, 26] were employed for this purpose. They are suitable for preparation of robust disposable or short-term-use sensors [27–31] and biosensors [21–23, 32–34]. These electrodes have similar electroanalytical properties to glassy carbon (GC) [25].

This work stems from previous studies on application of PNR as a redox mediator in biosensors, where a number of unanswered questions as to the role of PNR arose. It seeks to throw light on the mediation mechanism and PNR's electrochemical behaviour, in particular its dependence on the electropolymerisation method and experimental conditions.

Experimental

Reagents

Neutral red (NR) monomer— $N^8, N^8, 3$ -trimethylphenazine-2,8,-diamine (Fig. 1a)—was obtained from Aldrich (Ger-

many). Two oxysilane solutions were used as sol-gel precursors for enzyme encapsulation: 3-glycidoxypropyltrimethoxysilane (GOPMOS) and methyltrimethoxysilane (MTMOS) also from Aldrich. Glucose oxidase (GOx) from *Asperigillus niger*, EC 1.1.3.4, anhydrous α -D-(+)-glucose crystals, bovine serum albumin (BSA), and glutaraldehyde (GA) were obtained from Sigma (Germany).

Electrolyte solutions were 0.1 M phosphate buffer (PB) pH 5.5, prepared from sodium di-hydrogenphosphate and di-sodium hydrogenphosphate (Riedel-de-Haën), and 0.1 M phosphate buffer saline (PBS) pH 7.0 prepared from sodium di-hydrogenphosphate and di-sodium hydrogenphosphate (Riedel-de-Haën) with the addition of 0.05 M NaCl. Millipore Milli-Q nanopure water (resistivity $\geq 18 \text{ M}\Omega \text{ cm}$), and analytical reagents were used for preparation of all solutions. Experiments were performed at room temperature, $25 \pm 1 \text{ }^\circ\text{C}$.

Methods and instruments

A three-electrode electrochemical cell was used for cyclic voltammetry (CV) and electrochemical impedance spectroscopy (EIS) measurements. It contained a carbon film working electrode, without or with modification by PNR

and sol-gel encapsulated enzyme, a platinum (Pt) foil as counter electrode, and a saturated calomel electrode (SCE) as reference. Measurements were performed using a computer-controlled μ -Autolab Type II potentiostat/galvanostat with GPES 4.9 software (Eco Chemie, The Netherlands).

Electrochemical impedance measurements were carried out with a PC-controlled Solartron 1250 Frequency Response Analyser coupled to a Solartron 1286 Electrochemical Interface using ZPlot 2.4 software (Solartron Analytical, UK). A sinusoidal voltage perturbation of root-mean-square amplitude 10 mV was applied, scanning from 65 to 0.1 Hz with 10 points per frequency decade, integration time 120 s. Fitting to equivalent circuits was performed with ZView 2.4 software.

Electrode preparation

Electrodes were made from carbon film resistors ($\sim 2 \Omega$ resistance) [25, 26]. These resistors were fabricated from ceramic cylinders of external diameter 1.5 mm and length 6.0 mm by pyrolytic deposition of carbon. One of the tight-fitting metal caps, joined to a thin conducting wire, was removed from one end of the resistor, and the other was sheathed in plastic tube, gluing it with epoxy resin. In this way, the exposed cylindrical electrode geometric area was $\sim 0.20 \text{ cm}^2$. Before use, electrodes were electrochemically pre-treated by cycling the applied potential between 0.0 and +1.0 V vs SCE in 0.1 M KNO_3 solution for not less than 10 cycles, until stable cyclic voltammograms were obtained.

NR was polymerised electrochemically by cycling the applied potential between -1.0 and $+1.0$ V vs SCE at scan rate 50 mV s^{-1} for 20 cycles, or for 2 cycles followed by 18 cycles between -1.0 and $+0.55$ V vs SCE in a solution containing 1.0 mM NR monomer, 0.05 M PB pH 5.5 (in some cases 0.025 M PB pH 6.0 was used), and 0.1 M KNO_3 .

GOx was immobilised using GA cross-linking or sol-gel. In the former case, a mixture of 10 μl 10% GOx solution in 0.1 M PBS pH 7.0, 10 μl 10% BSA solution in 0.1 M PBS pH 7.0, 1 μl glycerol, and 1 μl 23% GA solution in water was prepared. A volume of 10 μl was then placed onto the electrode and allowed to dry at room temperature for at least 1 h. The sensors were stored in 0.1 M PBS at 4 °C when not in use.

The sol-gel solution was prepared by mixing GOPMOS, MTMOS, and water: 130:70:600 μl and adding 2 μl 6 M HCl, as in [23]. The mixture was intensively mixed for 2 min and then sonicated for 15 min to accelerate hydrolysis of the precursors. The alcohol formed during hydrolysis was removed by heating the solution at ~ 70 °C for approximately 30 min until the solution lost 40% of its volume. The solution was then cooled down and neutralised to pH 7 with 0.1 M NaOH solution. Fifty microlitres of the mixture was mixed with 15 μl of 10% GOx solution in

0.1 M PBS solution pH 7.0 and left for a few hours for gelation to start. When gelation began, PNR-coated carbon film electrodes were immersed in the sol-gel-enzyme solution for 5 min. then removed and left for sol-gel formation at 4 °C for 2–3 days. Biosensors were stored dry at 4 °C until first use.

Results and discussion

Poly(neutral red) electrodeposition

NR was polymerised by cycling the applied potential, as described in the experimental section, using one of two procedures:

1. Twenty potential cycles were carried out using the same potential window from -1.0 to $+1.0$ V vs SCE, i.e. enabling monomer oxidation to occur in all potential cycles, which is at approximately $+0.7$ V. This type of PNR-coated electrode will be referred to below as PNR (A).
2. Two cycles were performed from -1.0 to $+1.0$ V vs SCE, and all the following 18 potential cycles were reversed at $+0.55$ V positive potential limit before monomer oxidation could occur. This type of PNR-coated electrode will be referred to below as PNR(B).

Figure 2 shows CVs of NR polymerisation carried out both ways.

In Fig. 2a, the irreversible monomer oxidation wave at approximately $+0.7$ V vs SCE shifts with the number of scans to more positive potentials due to electrode surface changes caused by PNR film formation and pH alterations at the electrode surface. The redox couple centred between -0.6 and -0.5 V is due to NR-leuco-NR reduction-oxidation and shows polymer growth with an increasing number of cycles. The reduction peak shifts to more negative potentials with each cycle, and although after seven cycles, the reduction peak current starts to decrease, the potential continues to shift to more negative values, and the peak becomes broader. This could be related to branching of the PNR and changing of the surface structure. However, the oxidation peak increases constantly. The middle redox couple (doping and de-doping of the polymer) at 0.0 and $+0.2$ V increases much more slowly but linearly over the whole deposition time.

In Fig. 2b, when the positive potential limit was made less positive after two cycles, to avoid the formation of radicals by monomer oxidation and thence new polymer chains and to hinder polymer branching, no potential shift was observed in the polymer reduction peak nor any changes in peak shape. However, the peak current continued to increase a little as would be expected when

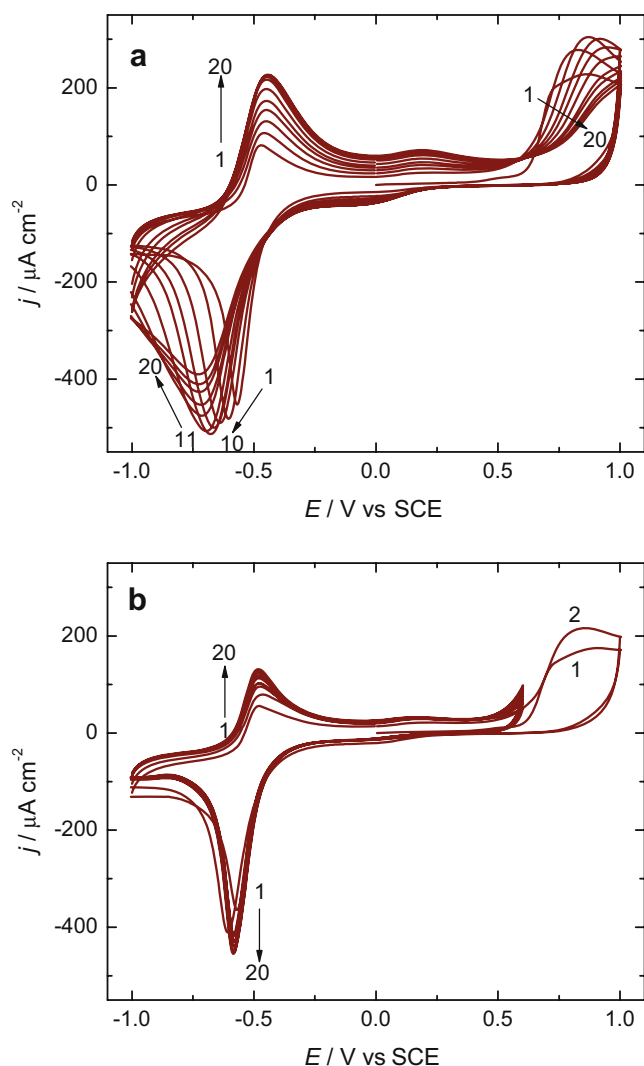


Fig. 2 Polymerisation of NR at carbon film electrode by potential cycling from a solution containing 1 mM neutral red, 0.05 M phosphate buffer, pH 5.5, and 0.1 M KNO_3 : **a** 20 cycles between -1.0 and $+1.0$ V vs SCE and **b** 2 cycles between -1.0 and $+1.0$ V followed by 18 cycles between -1.0 and $+0.55$ V vs SCE. Potential scan rate 50 mV s^{-1}

polymer growth is mainly one-dimensional and shows that some monomer was still left in the vicinity of the electrode surface and had not diffused into bulk solution.

To compare the influence of the electrode substrate, which could affect nucleation, on NR polymerisation, a film was also deposited using the second polymerisation procedure—PNR(B)—at a GC electrode. Deposition voltammograms (data not shown) looked very similar to those at carbon films. Although the peak current is initially much larger, it then increases more slowly, so that the current density during the last cycle is the same at both types of electrode substrate.

Previous work showed that on Pt [7], the polymerisation peak currents are smaller, and no peaks corresponding to nitrogen atom protonation–deprotonation were observed in

pH 1.0 solution. However, the negative potential limit was only -0.5 V vs Ag/AgCl due to hydrogen evolution. It is quite complicated to compare these results with the data presented in this work, as a much lower pH was used for PNR film formation. The authors showed that the potential of monomer oxidation and of the polymer redox couple shift towards 0.0 V with increase in pH, and the slope is ~ 60 mV per pH unit [7], as is also reported in [5].

NR was also polymerised at a Au electrode from the same solution using both polymerisation methods. The shapes of the deposition voltammograms (data not shown) looked rather similar to those at Pt [7], but no uniform film was obtained under these conditions.

Electrochemical characterisation of the PNR films

Carbon film electrodes with deposited PNR films were dried in air overnight, and cyclic voltammograms were then recorded in 0.1 M phosphate buffer, pH 5.5, see Fig. 3. At this pH, PNR exists in the protonated form, PNRH^+ , and is reduced to leuco-PNR, PNRH_3^+ [5]:



Both types of deposited PNR films, using narrower or wider potential windows, showed similar behaviour, except that in the case of PNR(A), the current density was higher than for PNR(B). PNR(B) deposited at GC had a significantly lower peak current, which suggests that PNR has a better adhesion at carbon film than at GC.

The polymer peak position and height depends on pH [5, 7, 9]. Cyclic voltammetry performed at PNR modified electrodes in 0.1 M Na PBS (pH 5.5; Fig. 4a) showed: a

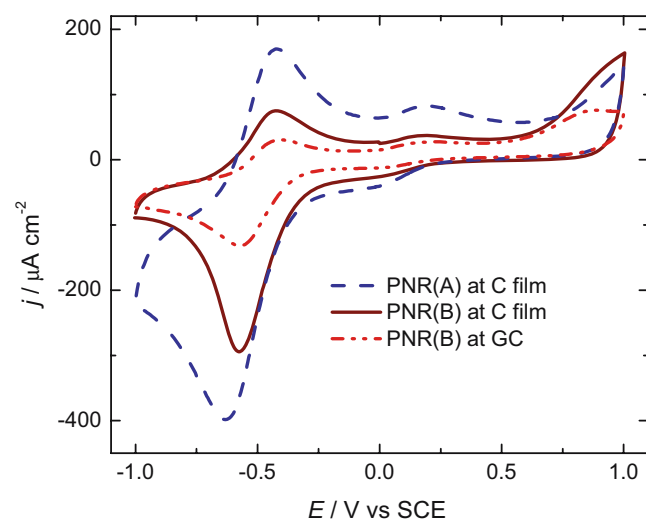


Fig. 3 Cyclic voltammograms, in 0.1 M phosphate buffer, pH 5.5, of PNR deposited at C film and GC electrodes using the two different polymerisation procedures, after drying overnight. Potential scan rate 50 mV s^{-1}

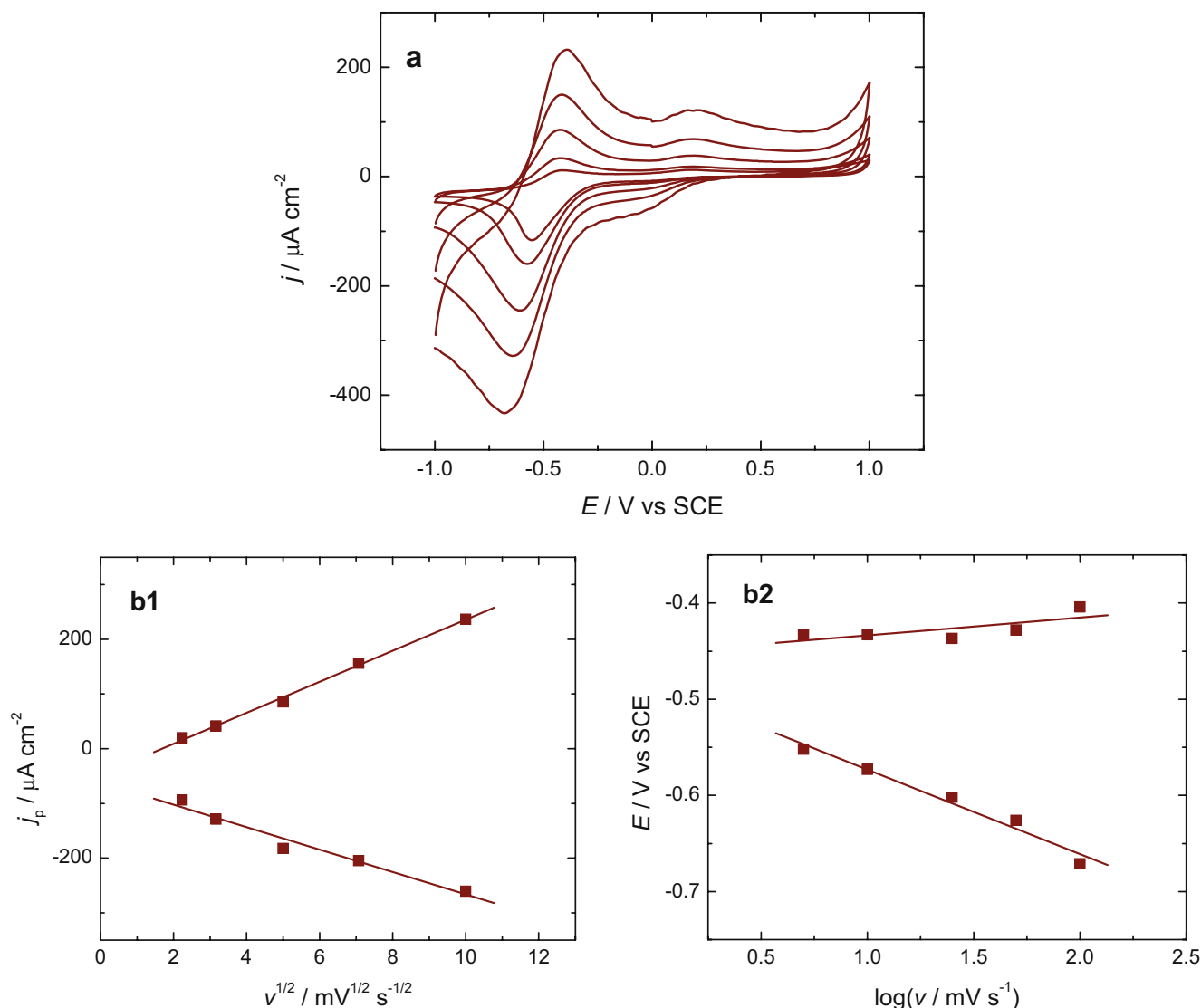


Fig. 4 a Cyclic voltammograms at PNR in 0.1 M PB, pH 5.5 at different potential scan rates: 5, 10, 25, 50, and 100 mV s^{-1} . b Dependence of peak currents on square root of potential sweep rate (1) and peak position on logarithm of sweep rate (2)

linear increase in peak current with square root of potential scan rate with a slope of 28.4 for the oxidation peak and of $-20.5 \text{ mV}^{1/2} \text{ s}^{-1/2} \mu\text{A}^{-1} \text{ cm}^2$ for the reduction peak (Fig. 4b1). This confirms that the electrochemical process at the PNR film is controlled by diffusion of the counter ion, as there is no monomer in the buffer solution.

A similar tendency was found for the dependence of the peak position on the logarithm of the scan rate, but the reduction peak shifted much more than oxidation (Fig. 4b2), as found during NR polymerisation, see previous section. At a sweep rate higher than 200 mV s^{-1} , the peaks became too broad to analyse.

EIS measurements were made to study the influence of PNR(A) films, i.e. at the films deposited using the wider potential window throughout the whole electropolymerisa-

tion process. The measurements were carried out in 0.1 M phosphate buffer solution pH 5.5 in 0.25 V intervals within the potential region from -1.0 to $+1.0 \text{ V vs SCE}$. Figure 5 shows complex plane impedance spectra at bare carbon film electrodes (black circles) and those modified with PNR (open circles) from -1.0 up to $+0.5 \text{ V}$. It was observed that impedance values are higher at PNR films at high positive or negative potentials, where the reduced form of PNR or the oxidised form of the NR monomer is predominant. At the potentials 0.0 and $+0.25 \text{ V vs SCE}$, the impedance spectra of the bare carbon film and PNR(A) are similar.

The spectra shown in Fig. 5 were fitted to electrical equivalent circuits. A model consisting of the cell resistance (R_{Ω}), in series with a charge transfer resistance, R_1 , connected in parallel with a constant phase element CPE_1 ,

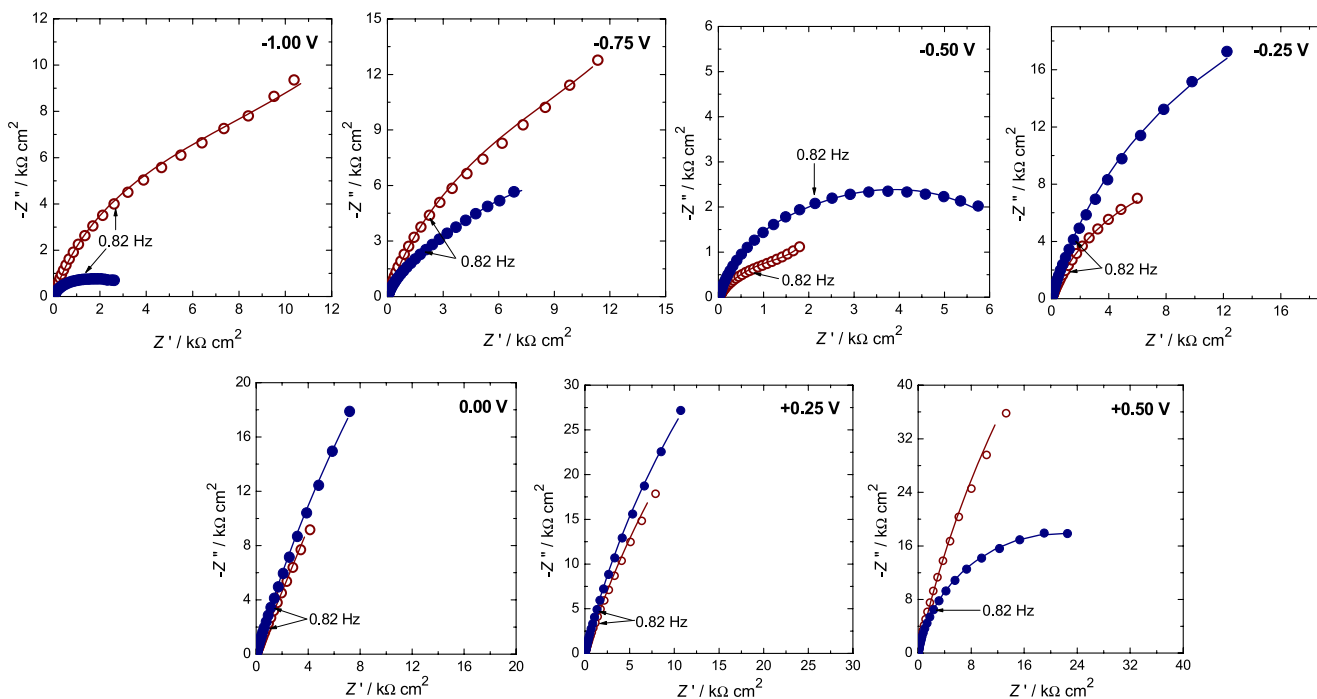


Fig. 5 Complex plane impedance spectra at bare carbon film (filled circle) and PNR film (open circle) at different applied potentials; the lines indicate fitted spectra. Supporting electrolyte 0.1 PB solution, pH 5.5. All other conditions in “Experimental”; potentials vs SCE

was used for spectra from -0.25 to $+1.0$ V vs SCE and represents the interface between the polymer film and the solution. The CPE was necessary due to the shape of the spectra and was considered as a non-ideal capacitance of capacity C with roughness factor α , where $\alpha=1$ represents a perfectly smooth surface. For the spectra at -1.00 , -0.75 , and -0.50 V, this circuit was extended with a second CPE₂– R_2 parallel combination in series, necessary to fit the low frequency part of the spectra at these potentials. Fitted values are given in Table 1. Cell resistance values were $\sim 11 \Omega \text{ cm}^2$ at the bare carbon film substrate and $\sim 13 \Omega \text{ cm}^2$ at carbon with PNR(A) films, independent of applied potential. In the case of the more positive potentials, the values of C_1 varied from 30 to $75 \mu\text{F cm}^{-2} \text{ s}^{\alpha-1}$ at bare carbon film and from 35 to $125 \mu\text{F cm}^{-2} \text{ s}^{\alpha-1}$ with the PNR film, showing some increase in charge separation, as could be expected. The charge transfer resistance, R_1 , is lowest around -0.5 V at the bare carbon film electrodes, due to surface oxide reduction and decreases again at -1.0 V, where some proton reduction begins to occur. The values of C_1 are clearly influenced by the presence of the PNR film. The values of R_2 , which in the case of the bare carbon electrode probably represent the residual oxide film, increase with the PNR film owing to its semiconducting nature at these potentials, although the values of C_2 remain similar. As most important conclusions, in the main range of interest for a biosensor, between -0.50 and 0.0 V, the PNR film shows a lower interfacial charge transfer resistance and a higher interfacial capacity.

Counter ions and pH have a strong effect on the electrochemical behaviour of PNR [7, 13, 14], which explains why the EIS data obtained by Benito et al. [13] in 0.1 M acetate buffer solution at pH 4.5 are significantly different from those reported in this work. However, when working in similar conditions, at pH 6.0, similar spectra were obtained [21].

Table 1 Data of the equivalent circuit fitting to the experimental impedance spectra in Fig. 5 at bare carbon film and at PNR(A) modified electrodes in 0.1 M phosphate buffer, pH 5.5

E/V vs SCE	$R_1/\text{k}\Omega \text{ cm}^2$	$C_1/\mu\text{F cm}^{-2} \text{ s}^{\alpha-1}$	α_1	$R_2/\text{k}\Omega \text{ cm}^2$	$C_2/\mu\text{F cm}^{-2} \text{ s}^{\alpha-1}$	α_2
Bare carbon film electrode						
-1.00	2.3	191.7	0.71	0.5	81.4	0.90
-0.75	18.6	132.2	0.75	1.6	93.4	0.87
-0.50	6.7	106.7	0.78	0.8	113.1	0.99
-0.25	56.1	57.9	0.83			
0.00	193.8	73.4	0.81			
+0.25	186.9	49.0	0.85			
+0.50	42.8	33.3	0.89			
PNR modified electrode						
-1.00	42.4	104.4	0.73	3.3	72.3	0.99
-0.75	92.5	92.9	0.74	3.9	89.4	0.99
-0.50	6.6	246.5	0.76	0.6	300.7	0.83
-0.25	23.5	124.3	0.78			
0.00	112.1	137.1	0.77			
+0.25	102.9	70.6	0.83			
+0.50	183.6	36.6	0.89			

Characterisation of the biosensor based on PNR-modified carbon film electrodes

PNR-modified carbon film electrodes were used to prepare biosensors to investigate the influence of the PNR deposition method on biosensor performance.

Enzyme entrapped in sol-gel (GOPMOS and MTMOS mixture 2:1) was applied on PNR-modified carbon film electrodes by dip coating. The PNR electrode was immersed in sol-gel-GOx solution for 5 min and was then taken out. The sol-gel solution had a slightly pink colour, which indicates that some of the film was dissolved in the sol-gel-GOx membrane on the electrode surface. The assembly was left for 3 days, and further characterisation was performed using CV and EIS.

A second type of biosensor with cross-linked GOx with GA was prepared by drop-coating using a GOx, BSA, and GA mixture as described in “[Experimental](#)”. Posterior examination of samples of the enzyme layer removed by peeling also showed a slight pink colour, indicating that some PNR had dissolved in the layer during biosensor preparation.

CVs were registered in 0.1 M PBS, pH 7.0, which is optimal for glucose electrochemical biosensor activity. Using the PNR deposited by potential cycling from -1.0 to $+1.0$ V vs SCE over the whole deposition time, PNR(A), the redox peaks are smaller than at pH 5.5, but they are still approximately at the same position. The peaks are misshapen and smaller by almost a factor of two compared to PNR(A) before sol-gel deposition, due to the diffusion barrier created by the rather thick sol-gel layer. No difference was obtained in the CV at PNR/sol-gel without or with GOx. With respect to the GA cross-linked GOx membrane, which was thinner, the peak current density remained the same as at bare PNR(A). The same trends were found using PNR(B) (not shown).

Impedance spectra were registered in the negative potential region at three values, where the response of the biosensor is best, at PNR, and at PNR with sol-gel layer with and without enzyme. EIS measurements with GA cross-linked enzyme have been performed in previous work [21]. The spectra showed a general increase in impedance values after sol-gel layer deposition on the PNR film, particularly at -0.5 V vs SCE, indicating that the sol-gel layer caused an increase in the charge transfer resistance of the film. Values of parameters obtained from analysis of the spectra are presented in Table 2, using the same model as for PNR films. Surprisingly, after sol-gel application on top of the PNR film, the cell resistance increased to $\sim 30 \Omega \text{ cm}^2$, but with enzyme entrapped in sol-gel, the cell resistance again decreased and was even lower than at PNR films without a sol-gel layer. The charge transfer resistance R_1 remains almost the same at the potentials studied and is also

Table 2 Data of the equivalent circuit fitting to impedance spectra at PNR films coated with GOPMOS–MTMOS sol-gel and with GOx immobilised in the same sol-gel

E/V vs SCE	$R_1/k\Omega \text{ cm}^2$	$C_1/\mu\text{F cm}^{-2} \text{ s}^{\alpha-1}$	α_1
PNR/sol-gel			
-0.50	49.2	141.2	0.71
-0.25	49.0	78.8	0.75
0.00	43.7	67.7	0.73
PNR/sol-gel-GOx			
-0.50	4.0	157.8	0.77
-0.25	9.7	137.6	0.94
0.00	7.1	533.8	0.99

Spectra were recorded in 0.1 M phosphate buffer, pH 7.0.

higher at the sol-gel film without encapsulated enzyme. The capacitance is higher at the enzyme-containing films. These results are similar to those obtained using enzyme layers with GOx encapsulated by GA cross-linking [21].

These data indicate clearly that the sol-gel layer structure is different with and without enzyme, so that care must be taken in extrapolating results obtained with sol-gel layers without enzyme to those where enzyme is encapsulated. Indeed, the sol-gel with GOx enzyme can be assumed to have a more open structure, although such differences are not visible in the CVs at PNR/sol-gel and PNR/sol-gel-GOx. Moreover, different enzymes can influence the structure and EIS spectra in different ways, as shown for glucose and pyruvate oxidases with GA cross-linking in [21].

Performance of the biosensor

PNR-modified electrodes were first used to detect hydrogen peroxide in amperometric mode at -0.25 V vs SCE in 0.1 M PBS (pH 7.0), and the response was an increase in cathodic current with addition of hydrogen peroxide (data not shown). This suggests that, at this applied potential, hydrogen peroxide is reduced at the PNR electrode.

To see the response to glucose at a GOx biosensor with PNR(A) as redox mediator, chronoamperograms were recorded at the same potential of -0.25 V vs SCE in 0.1 M PBS, (pH 7.0) with standard additions of 0.1 M glucose stock solution. Figure 6 shows a typical calibration curve for glucose at a PNR(A)-mediated biosensor. However, the response was an anodic change in current, which suggests that an oxidation process occurs at the electrode. The reaction mechanism proposed involves flavin adenine dinucleotide (FAD) regeneration by PNR(ox) and is presented in Scheme 1 and explains the typical Michaelis–Menten behaviour in the case of cross-linked enzyme. However, at the sol-gel biosensor, the calibration plot exhibited two linear ranges, so that the mediation mecha-

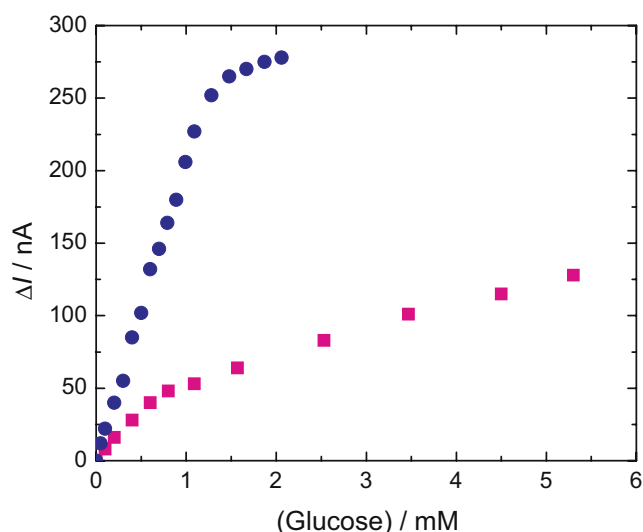


Fig. 6 Calibration curves for glucose at (circle) PNR/GOx-BSA-GA and (square) PNR/sol-gel-GOx in 0.1 M PBS solution, pH 7.0. Applied potential -0.25 V vs SCE

nism is more complicated and could result from competition between regeneration of FAD at the PNR (Scheme 1a) and hydrogen peroxide detection (Scheme 1b).

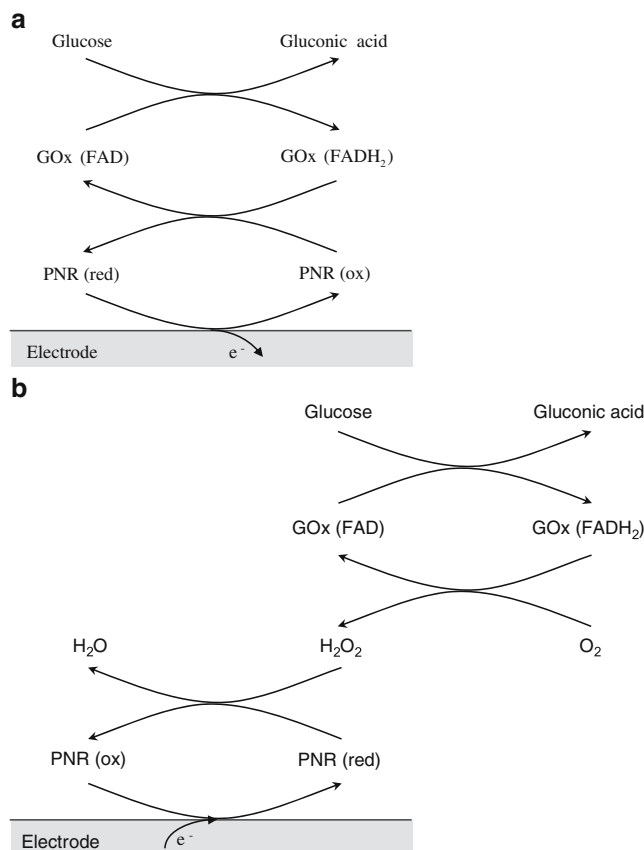
Experiments performed with enzyme and monomer in solution with and without O_2 showed that, in the presence of oxygen, the biosensor exhibited a lower sensitivity, which supports the hypothesis that there is a competition between hydrogen peroxide reduction and $FADH_2$ oxidation. In the presence of oxygen, the total current measured is the sum of the values of currents obtained from the two competitive reduction and oxidation processes. When oxygen is removed, no hydrogen peroxide should be produced by the enzyme reaction, so that there is only $FADH_2$ oxidation at PNR, and the measured current is more anodic.

To cast further light onto the question as to which process, hydrogen peroxide reduction (Scheme 1b) or FAD regeneration at PNR (Scheme 1a), occurs, the buffer solution was deoxygenated by bubbling of N_2 . It was found that the background current at the PNR biosensor in deoxygenated buffer solution is much closer to zero, and biosensor stabilisation took significantly longer. The results of the response to glucose with and without oxygen are presented in Fig. 7. As seen from Fig. 7a, in the presence of oxygen, the sol-gel biosensor is more sensitive and responds to a smaller amount of analyte as well as having a much shorter linear range. After deoxygenation, a linear range is obtained up to 12 mM of glucose, but at the same time, the biosensor also starts to respond only at rather high analyte concentrations, and the sensitivity is lower. This cannot be due to enzyme deactivation because when a new calibration curve was recorded in solution without oxygen removal, the same calibration curve as before with higher

sensitivity was obtained. It is therefore likely that at low glucose concentrations, hydrogen peroxide is detected, and at higher ones, regeneration of FAD at PNR can also occur. The difference in behaviour, with and without oxygen in solution, is probably due to the rather thick sol-gel layer.

In the case of the biosensor with GOx cross-linked with GA, after oxygen removal, the same response was found at low glucose concentrations, but it decreased with increase in analyte concentration, and the linear range was shorter (Fig. 7b). The membrane of the cross-linked enzyme is thinner than the sol-gel membrane, and therefore, electron transport could occur more easily than at the sol-gel biosensor, so that oxygen has less influence. Nevertheless, the pinkish colour of the GA layer, as mentioned previously, suggests that NR monomer or oligomers are present to aid electron conduction.

The nature of the enzyme also plays an important role in the process at PNR-mediated biosensors. For example, it was reported in [21] that in the case of pyruvate oxidase, when pyruvate is the analyte, H_2O_2 reduction occurred at the electrode because a cathodic current was recorded at



Scheme 1 Proposed reaction mechanisms at the PNR-based biosensor for **a** regeneration of FAD and **b** hydrogen peroxide detection

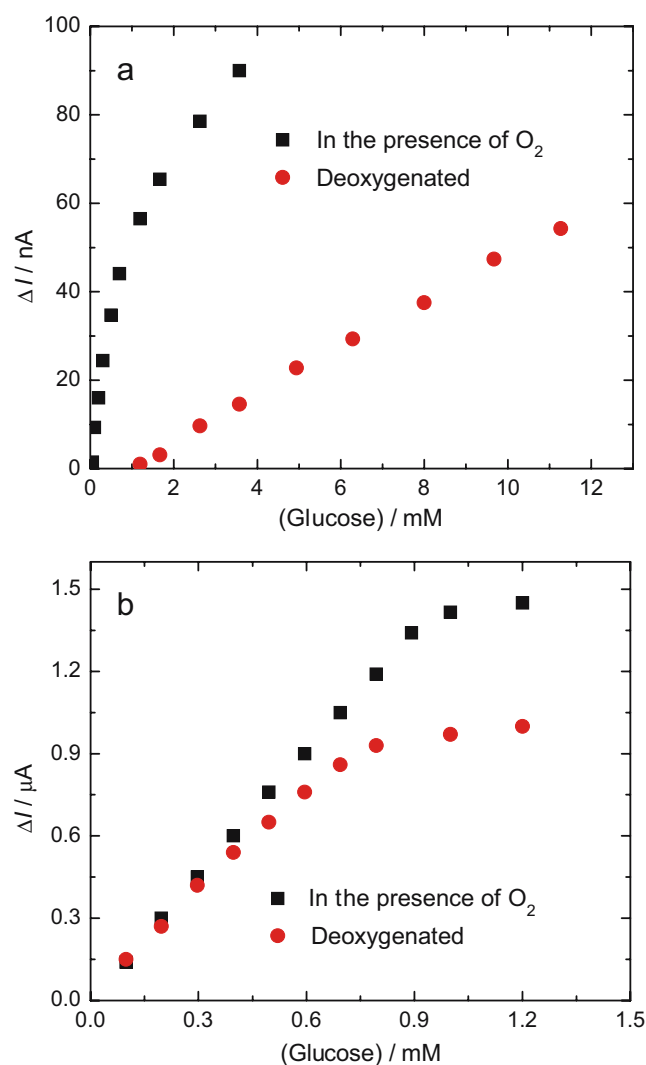


Fig. 7 Calibration curves for glucose at **a** PNR/sol-gel-GOx and **b** PNR/GOx-BSA-GA in 0.1 M PBS solution, pH 7.0, in the presence and absence of oxygen. Applied potential **a** -0.25 and **b** -0.35 V vs SCE

-0.25 V vs SCE in trizma-HCl buffer solution (0.01 M trizma-HCl + 0.05 M KCl + 0.015 K_2HPO_4), pH 7.2.

To investigate if monomer/oligomer dissolution into the enzyme layer affects the biosensor performance, two biosensor assemblies were compared: one with a PNR film kept for 6 days in buffer solution before making the enzyme layer and the other containing PNR without storing in buffer. In the former case, some leaching of monomer from the PNR film into the buffer occurred, shown by the pink colour, but even after this pre-treatment, the enzyme layer still presented a pink colour. The response of this biosensor was slightly higher compared with the biosensor response containing PNR without being stored in buffer, probably due to an increase in active surface of the PNR because the film became swollen and had a more porous structure.

Finally, the influence of the PNR deposition method on biosensor performance was studied at PNR-mediated biosensors. The polymer structure had no significant influence, especially at low analyte concentrations. The sensitivity at the different biosensors was ($nA\ mM^{-1}$): 206 ± 3 at PNR(A)/GOx-BSA-GA, 177 ± 3 at PNR(B)/GOx-BSA-GA (at -0.25 V vs SCE), 594 ± 8 at PNR(A)/sol-gel-GOx, and 712 ± 4 at PNR(B)/sol-gel-GOx, ($n=3$; at -0.35 V vs SCE). At the GA cross-linked biosensor, there is an approximately 14% reduction in sensitivity with the thinner, more linear polymer structure, but there is an approximately 20% increase at the sol-gel biosensor, perhaps due to easier dissolution of the more linear polymer in the sol-gel. Nevertheless, the relatively similar sensitivities suggest that the polymer thickness and structure does not result in much better contact with the active part of the enzyme.

Additionally, the mediation mechanism does not depend on the PNR polymerisation potential window, confirmed by carrying out the same series of experiments for glucose determination with and without solution deoxygenation at PNR(B)-mediated biosensors. The results obtained were very similar to those obtained at PNR(A) (Fig. 7), except that in the case of the PNR(B)/sol-gel-GOx biosensor in the absence of O_2 , the biosensor responded to lower glucose concentrations, but the sensitivity was three times lower than in the presence of oxygen, and the linear range was up to 3 mM glucose.

Conclusions

The polymer redox mediator, PNR, was prepared by electropolymerisation on carbon film electrodes and characterised electrochemically to ascertain the best conditions for effective mediation in sol-gel-based enzyme biosensors and to clarify the mediation mechanism.

It was found that the electrochemical properties of PNR depend on the applied potential cycling scheme during electropolymerisation, as is the case with many conducting polymers, and on whether the substrate is carbon film or GC electrodes. When the monomer can be oxidised throughout the potential cycling, the electrochemical properties of the resulting polymer show noticeable differences compared with when monomer oxidation is impeded after the first two cycles by reducing the positive potential limit.

Glucose biosensors with PNR redox mediator and immobilised GOx show a mechanism that comprises two processes involving hydrogen peroxide reduction and regeneration of FAD co-factor by oxidation at PNR. The results of this competition can depend on the nature of the enzyme and, thus, influence the observed mediation

mechanism. The type of PNR film, of the two tested, hardly influences biosensor performance. Sol-gel slightly dissolves PNR during the coating procedure and so distributes it in the bulk sol-gel enzyme layer allowing an easier path for electron transfer and facilitating hydrogen peroxide reduction; this dissolution also occurs in the cross-linked GA enzyme layer. Because the sol-gel entrapped enzyme layer is thicker than that using cross-linking with GA, these effects are more noticeable.

Acknowledgements Financial support from Fundação para Ciência e Tecnologia (FCT) Portugal. R.P. thanks FCT for a Postdoctoral fellowship (SFRH/BPD/14518/2003) and M.E.G. for a Ph.D. grant (SFRH/BD/14014/2003). Prof. H.-D. Liess is thanked for the gift of the electrical resistors.

References

1. Guttenberg M (2000) *Plant Soil* 226:211
2. Cardona PJ, Soto CY, Giquel B, Augustí G, Guirado E, Sirakova T, Kolattukudy P, Julián E, Luquin M (2006) *Microbes Infect* 8:183
3. Ricci V, Sommi P, Fiocca R, Necchi V, Ramano M, Solcia E (2002) *Biochem Biophys Res Commun* 292:167
4. Ni Y, Lin D, Kokot S (2006) *Anal Biochem* 352:231
5. Halliday CS, Matthews DB (1983) *Aust J Chem* 36:507
6. Choi JP, Bard AJ (2004) *J Electroanal Chem* 573:215
7. Chen SM, Lin KC (2001) *J Electroanal Chem* 511:101
8. Schlereth DD, Karyakin AA (1995) *J Electroanal Chem* 395:221
9. Karyakin AA, Bobrova OA, Karyakina EE (1995) *J Electroanal Chem* 399:179
10. Karyakin AA, Karyakina EE, Schmidt HL (1999) *Electroanalysis* 11:149
11. Kubota LT, Gorton L (1999) *Electroanalysis* 11:719
12. Inzelt G, Csahók E (1999) *Electroanalysis* 11:744
13. Benito D, Gabrielli C, García-Jareño JJ, Keddam M, Perrot H, Vicente F (2002) *Electrochem Commun* 4:613
14. Benito D, Gabrielli C, García-Jareño JJ, Keddam M, Perrot H, Vicente F (2003) *Electrochim Acta* 48:4039
15. Chen SM, Fa YH (2003) *J Electroanal Chem* 553:63
16. Karyakin AA, Ivanova YN, Karyakina EE (2003) *Electrochem Commun* 5:677
17. Tang X, Fang C, Yao B, Zhang W (1999) *Microchem J* 62:377
18. Sun Y, Ye B, Zhang W, Zhou H (1998) *Anal Chim Acta* 363:75
19. Broncová G, Shishkanova TV, Matějka P, Volf R, Král V (2004) *Anal Chim Acta* 511:197
20. Sun W, Jiao K, Han J, Lu L (2005) *Anal Lett* 38:1137
21. Ghica ME, Brett CMA (2006) *Electroanalysis* 18:748
22. Ghica ME, Brett CMA (2006) *Anal Lett* 39:1527
23. Pauliukaite R, Chiorcea Paquim AM, Oliveira Brett AM, Brett CMA (2006) *Electrochim Acta* 52:1
24. Qu F, Yang M, Chen J, Shen G, Yu R (2006) *Anal Lett* 39:1785
25. Brett CMA, Angnes L, Liess HD (2001) *Electroanalysis* 13:765
26. Filipe OMS, Brett CMA (2004) *Electroanalysis* 16:994
27. Filipe OMS, Brett CMA (2003) *Talanta* 61:643
28. Gouveia-Caridade C, Brett CMA (2005) *Electroanalysis* 17:549
29. Pauliukaite R, Brett CMA (2005) *Electroanalysis* 17:1354
30. Pauliukaite R, Florescu M, Brett CMA (2005) *J Solid State Electrochem* 9:354
31. Gouveia-Caridade C, Brett CMA (2006) *J Electroanal Chem* 592:113
32. Florescu M, Brett CMA (2004) *Anal Lett* 37:871
33. Florescu M, Brett CMA (2005) *Talanta* 65:306
34. Ghica ME, Brett CMA (2005) *Anal Chim Acta* 532:145